'94 KACC (1994. 10. 17 ~ 20)

Failure Detection of Indexing Drive by Vibration Measurement

Masayuki Yokoi, Junior College, Osaka Sangyo University, 3-1-1, Nakagaido, Daito-shi, Osaka, 574, Japan
Koichiro Obara and Hiromitsu Ohara, Japan Tobacco LTD.
Mikio Nakai, Kyoto University

Abstract

Wrapping machines in cigarette factories are equipped with indexing drive units with roller gear cam. At present there are no simple, visual, diagnostic techniques for predicting failure in these units at an early stage. This paper proposes that failure could be predicted by using either a modified version of kurtosis, or the Wigner distribution method. The nonlinear vibration model proposed in this paper takes into consideration the play between the cam and the cam follower, and precisely simulates the actual vibration. Statistics on the variance in play, obtained from the data on time history, can then be used to evaluate the effects of the damage on the cam and cam follower.

1. Introduction

There are many types of indexing drive units which produce intermittent movement. Indexing drive units with roller gear cam are often used in rotating machines because of their numerous advantages including high stiffness, high rotational speed, and mechanism without play. In particular, the indexing drive units in cigarette factory wrapping machines produce precise, intermittent movement with roller gear cam, and are capable of high rotational speeds. Although indexing drive units generally have excellent durability, even occasional failure can interfere with production. Currently, neural network techniques or acoustic emission (A.E.) methods are used as diagnostic tools to monitor the performance of these machines;[1]-[3] however, a simpler diagnostic tool would be more effective. This paper proposes such a technique using vibration measurement.

2. Experimental apparatus and setup

The experiment was performed on an isolated indexing drive unit. The setup of the apparatus is shown in Fig.1. The indexing drive unit is driven by belts and a flywheel is mounted on the output shaft as a load. Figure 2 illustrates schematically the mechanism of the roller gear cam assembled in the driving unit, as well as the motion of the cam follower projected onto a plane during one revolution of the roller gear cam.

The output shaft indexes and dwells during each revolution of the input shaft. When the output shaft is in index, the cam followers engage the helical track of the taper rib, and the output shaft rotates. When the output shaft is in dwell, the cam followers engage the straight track of the taper rib, and the output shaft does not move. The experimental indexing drive unit performs one index(0-120°) and one dwell (120-360°) during each revolution (0-360°) of the input shaft. The output shaft rotates 60° when it is in index, and makes one revolution every 6 revolutions of the input shaft.

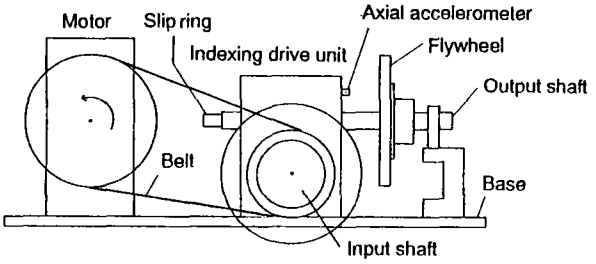

Fig.1 Experimental apparatus

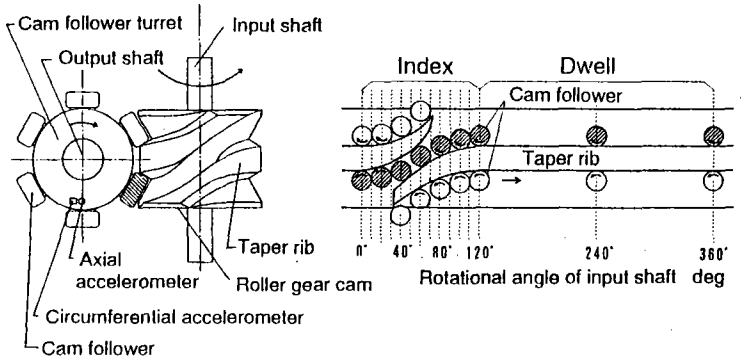

Fig.2 The mechanism of the roller gear cam assembled in the driving unit and the motion of the cam follower projected onto a plane during one revolution of the roller gear cam

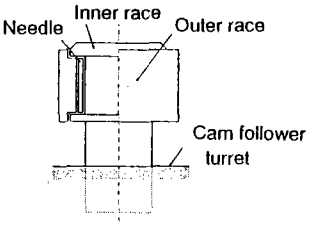

Fig.3 The construction of needles bearings

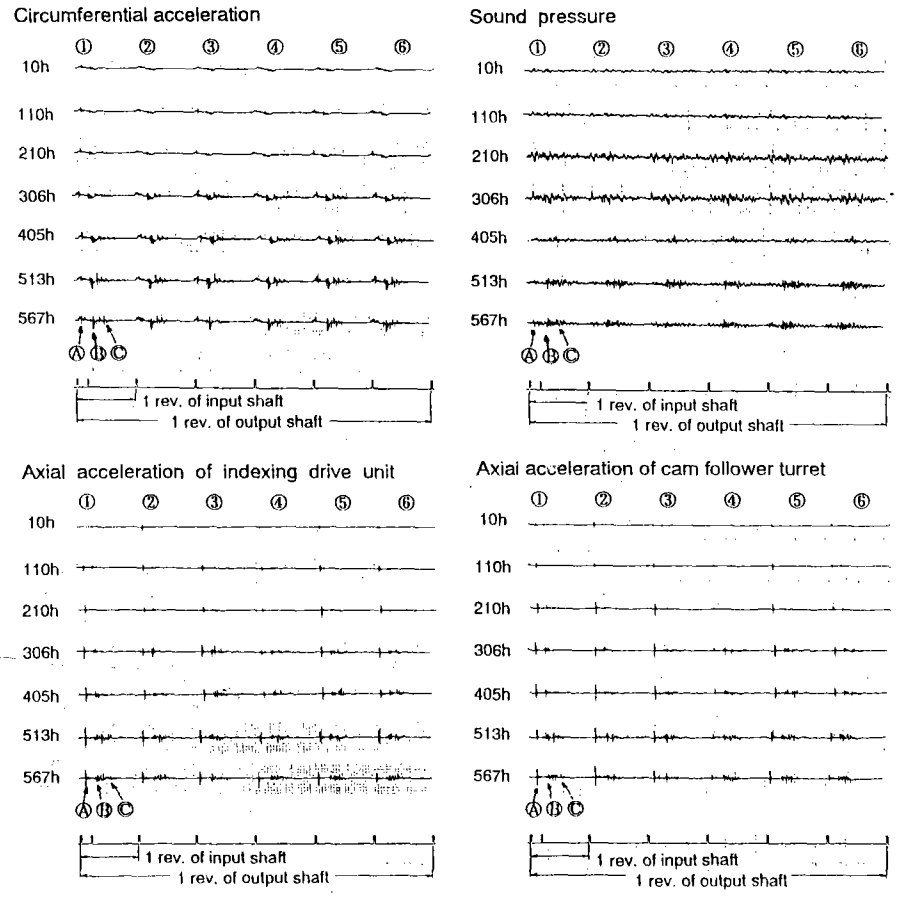

Fig.4 Four kinds of time histories versus operation time

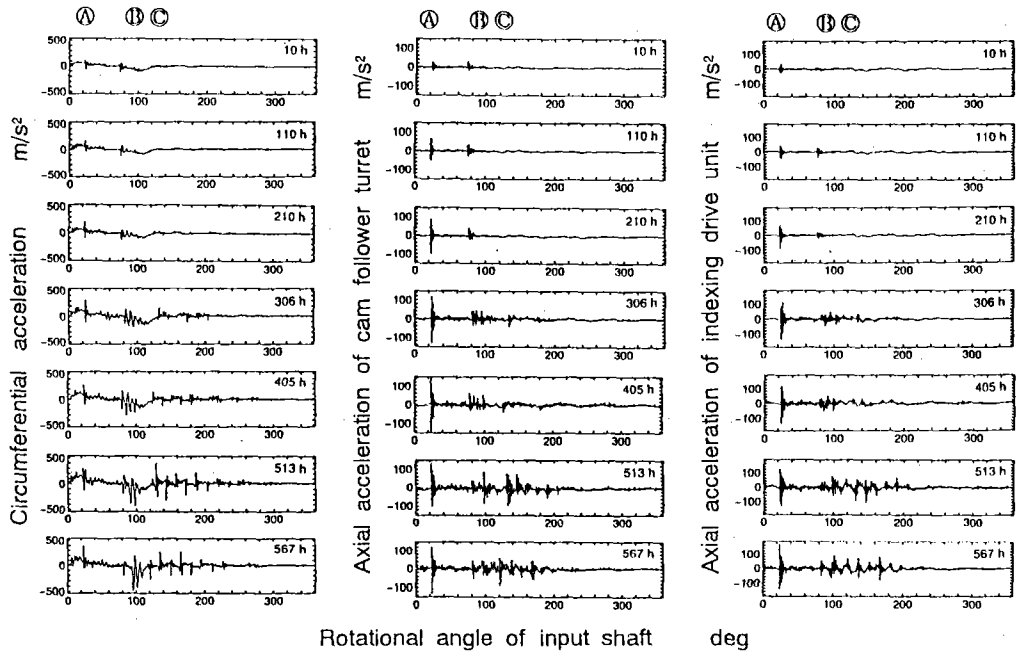

Fig.5 The enlarged acceleration time histories for the cam follower ① during one revolution of the input shaft

When the output shaft is in dwell, the preload can be applied between the cam follower and the roller gear cam by adjusting the distance between the input/output shaft. If the cam follower (the shaded area in Fig.2) rotates anti-clockwise at the beginning of the index, then it rotates clockwise at the end. Play between the cam follower and the taper rib is made approximately midway through the index, which allows for reverse rotation of the cam follower. At this point, the rotational speed of the output shaft stops increasing and begins to decrease.

There are needle bearings between the outer/inner race of the cam follower, as shown in the enlarged sectional view in Fig.3. Frequent collision of the cam follower with the taper rib produces the damage of the needle bearings. This is the most common cause of failure in the indexing drive unit.

Sound and accceleration measurements were taken for the purpose of obtaining diagnostic signals. The accelerations were measured with accelerometers (Bruel & Kjaer type 4393), which were placed at the cam follower turret in both circumferential and axial directions. The signals were taken out through a slip-ring. In order to monitor operating conditions of the indexing drive unit easily, another accelerometer was positioned at the housing of the indexing drive in the axial direction of the output shaft.

Sound pressure was measured with 1/2 inch microphone (B&K 4165, microphone amplifier, B&K 2607) at a distance of approximately 200 mm from the housing in the direction of the output shaft. The endurance test for the indexing drive was performed at a constant of 600 rpm. At the same time, the dynamic behavior of the indexing drive and the sound which radiated from it were measured at regular intervals.

3. Experimental results

3.1 Time history versus operation time: Figure 4 shows four kinds of time histories in relation to operation time; accelerations in both the circumferential and axial directions of the cam follower turret, acceleration in the axial direction at the housing of the indexing drive, and sound pressure. The circled numbers ①-⑥ indicate the number of the cam follower. The amplitudes of impulsive signals Ⓐ and Ⓑ in all accelerations increase with operation time. Impulsive signal Ⓒ only appears after 306 hours of operation in all accelerations, and increases from there. In the axial accelerations at the cam follower turret and the housing, the amplitude of impulsive signal Ⓐ of the cam follower ④ is less than that of the other cam followers. The significance of this will be discussed at the end of this section.

The purpose of this experiment was to find a precise relationship between acceleration time history and the mechanism of the indexing drive. Sound pressure time histories cannot be used for this purpose because they do not exhibit distinct trends, as other sounds are mixed in with the measurements. As a result, acceleration time histories were used instead. Figure 5 shows the enlarged acceleration time histories for one revolution of cam follower ①. Figure 6 shows the relation between the time history of vibration and the motion of cam follower. The path which the cam follower makes as it completes one revolution of the roller gear cam has been projected onto a plane in the center of the figure. As mentioned above, the output shaft performs one index and one dwell for each revolution of the input shaft. Figs.5 and 6 show the original locations and causes of peaks Ⓐ – Ⓒ. Peak Ⓐ occurs around the beginning of the index and is generated by the first impulse between the cam follower and the taper rib. Peak Ⓑ occurs midway through the index, when the cam follower reverses direction. As operation time increases, there is also an increase in play between the cam follower and the taper rib, which produces impulsive vibrations. Peak Ⓒ occurs at the point where the index changes to the dwell. Since high frequency components (impulsive vibrations) do not occur in the early stages of operation, it should be noted that they are generated by continual wear on the roller gear cam and the cam follower, and/or by an increase in play in the rotating body. Thus, there is a correlation between indexing drive failure and variations in amplitude for peaks Ⓐ and Ⓒ. Furthermore, the axial acceleration time histories at the housing resemble those at the cam follower turret. Since the axial acceleration at the housing can be measured more easily, it is henceforth utilized for analysis purposes in this paper.

3.2 The acceleration time history in failure: After 567 hours of operation, the indexing drive began to display intermittent periods of inactivity. The sound pressure level decreased suddenly as well. The indexing drive looked as if it were no longer revolving, and operation was halted. Figure 7 compares the circumferential and axial acceleration time histories during this period with those of normal operation. When the indexing drive is in a period of inactivity, the amplitude of peak Ⓐ decreases. The increase in play between the cam and the cam follower relieves the engaging shock, at which point both vibration and sound pressure levels decreases. Therefore, it is possible to conclude that there is a correlation between abnormal vibration and a failure in the indexing drive unit.

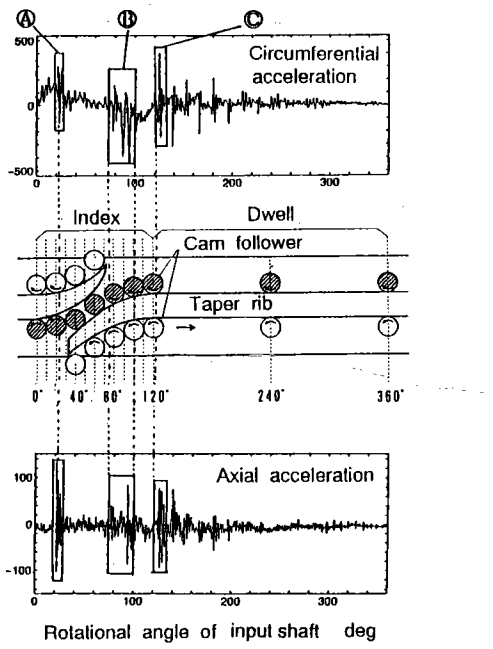

Fig.6 The relation between the time history of vibration and the motion of cam follower

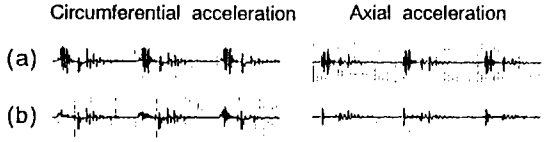

Fig.7 The circumferential and axial acceleration time histories (a): in normal operation and (b): in displaying intermittent periods of inactivity.

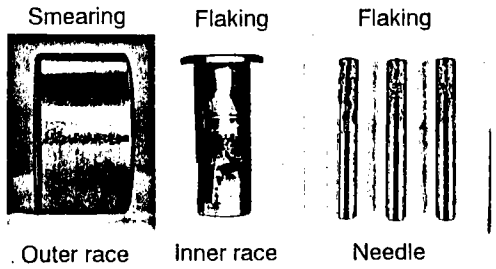

Fig.8 The photos of the outer, inner races as well as needles of cam follower ④, which suffered serious damage.

3.3 Dismantling of the indexing drive unit: After the above abnormal vibration occurred, the indexing drive unit was dismantled and examined. Figure 8 shows photos of both the inner and outer races, as well as the needles of cam follower ④, which suffered serious damage. In addition, smearing was observed on the surface of the outer race. This was most likely generated by either insufficient cooling or poor lubrication for abnormally high heating in bearings, due to irregular contact with the race. Flaking was found on the inner race and the needles. Furthermore, the surfaces of needles are exfoliated, most likely because a heavy load had been applied to needles when the output shafts was in index.[4] It can be predicted that the needles of the cam follower would soon be broken with higher revolution and/or a heavier load than the rate.

Smearing and serious damage produced by impulsive forces was also observed on the surface of the roller gear cam (no photo available). The acceleration amplitude increased when the damage to roller gear cam was more serious. Since the cam was worn down by high revolutions and a heavy load, the preload between the cam and the cam follower decreased. Therefore, it is assumed that high frequency components would most likely be generated in acceleration. Finally, it was noted earlier that the amplitude of impulsive peak Ⓐ in the axial acceleration of cam follower ④ was lower than that of the other cam followers. Since this cam follower also suffered damage, it can be concluded that detecting abnormalities in the first impulsive peak of the time history in the axial acceleration of the output shaft is a good predictor of damage.

4. Analysis of experimental results

4.1 Time domain analysis techniques: Numerous magnitude and time domain techniques are available for vibration diagnostics. The analysis of the individual time histories of vibration signals is in itself a very useful diagnostic procedure. Several magnitude parameters can be extracted from the time history of vibration, including variance, r.m.s. level, absolute mean value, maximum value, the crest factor and kurtosis. Kurtosis, the fourth statistical moment, is widely used in machinery diagnostics, particularly with rolling element bearings. Figure 9 shows trends of these statistical magnitude parameters for circumferential and axial accelerations with respect to operation time. Based on the figures, the followed can be discerned: (1) the parameters for circumferential acceleration vary more than those for axial acceleration; (2) the variance, the r.m.s. value, the absolute mean value and the maximum value increase with operation time; (3) the crest factor stays almost constant regardless of operation time; and (4) for circumferential acceleration, kurtosis increases suddenly just prior to failure of the indexing drive unit, but with axial vibration, it reaches a peak at 200 hours and then decreases.

A simple diagnostic tool should have either a statistical

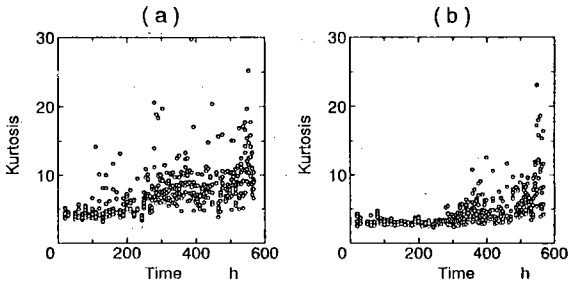

Fig.10 Kurtosis values of axial acceleration calculated for (a): the time history omitting peak Ⓐ and (b): the time history omitting peaks Ⓐ and Ⓑ

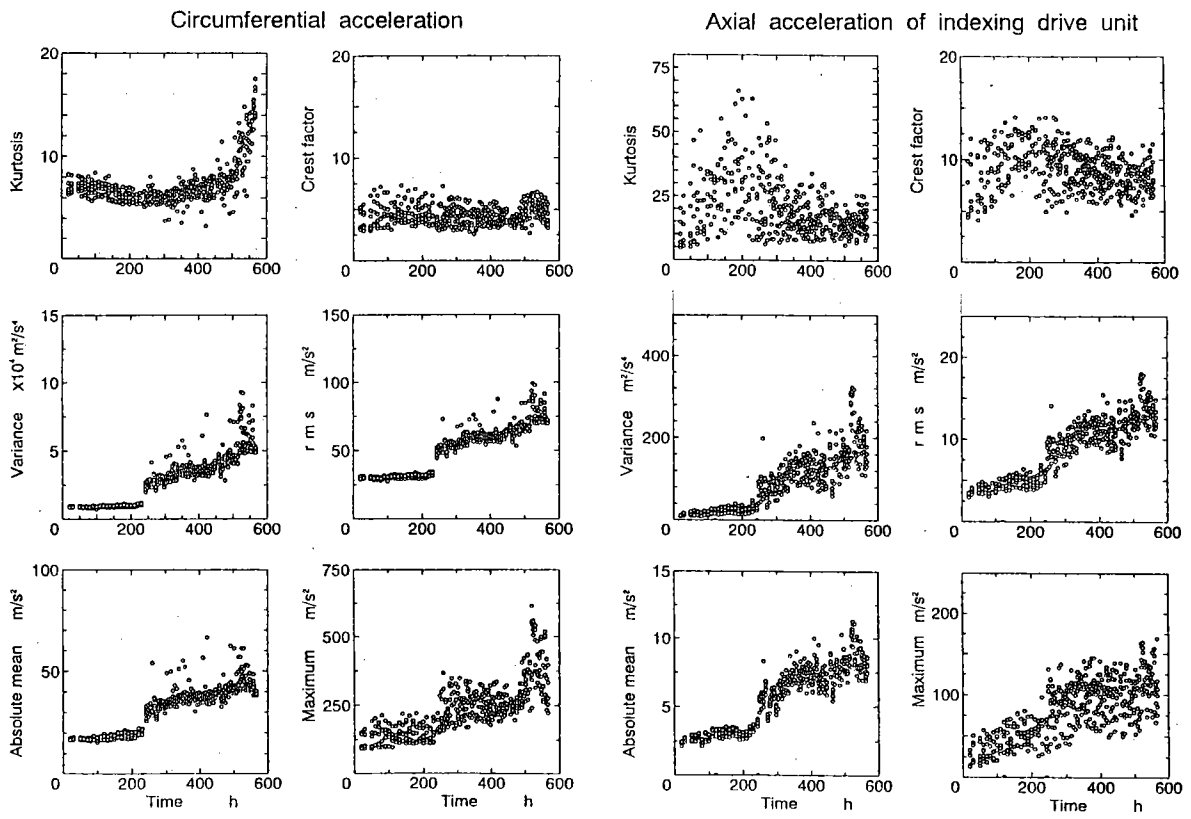

Fig.9 The trends of various statistical parameters of the circumferential and axial accelerations with operation time

parameter with identifying marks such a sudden change in trend after a given/specified period of operation, or a signal which can be easily measured on the surface of the housing. With these factors in mind, we will now discuss the appropriateness of using variance and kurtosis as simple diagnostic tools.

First, it is true that variance increases just before failure. However, variance may also fluctuate for other reasons; furthermore there is no strong correlation between the rate of variance and operation time.

Next, although kurtosis for circumferential acceleration provides a clear signal, it is not easy to measure. Furthermore, kurtosis for axial acceleration can not be utilized to detect failure as it is because it reaches its maximum value before failure, and it indicates the amount of scatter, which makes it difficult to detect a clear trend. In general, kurtosis is reliable only in the presence of significant impulsiveness, caused by flaking of the bearing. In Figs. 4 and 5, impulsive peaks Ⓐ and Ⓑ were present in the axial vibration from the beginning of operation time. Kurtosis values were calculated twice: the first time omitting peak Ⓐ, and the second time omitting peaks Ⓐ and Ⓑ. The results are shown in Figs 10(a) and (b) respectively. In Fig. 10(b), kurtosis value increases suddenly after 500 hours of operation as shown in circumferential acceleration in Fig.9.

Thus, variance is not an appropriate diagnostic tool because it does not exhibit distinct trends. However, kurtosis can be used as diagnostic tool if peaks Ⓐ and Ⓑ are omitted from analysis. Next, the Wigner distribution method will be considered.

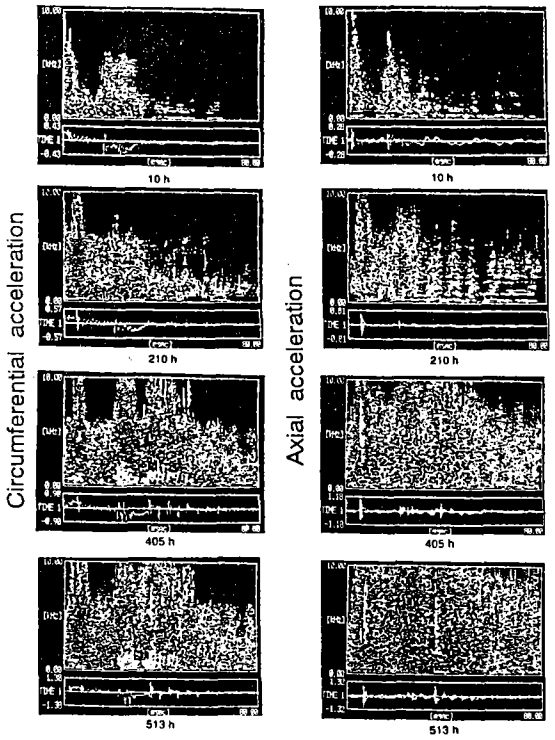

Fig.11 Wigner distributions for circumferential and axial vibrations at different operation times

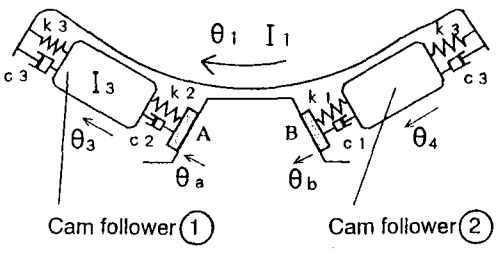

Fig.12 The physical model for circumferential vibration in order to investigate the influence of preloading or play between the cam and the cam follower in acceleration time history

4.2 Frequency domain analysis technique (Wigner distribution): The impulsive vibration of the indexing drive would produces a transient change in the frequency spectrum which can be easily identified by analyzing one revolution of the input shaft using the Wigner distribution method. Figure 11 shows Wigner distributions for circumferential and axial vibrations at different operation times. The light and dark areas indicate the magnitude of the acceleration level. The light areas indicate a high level and the dark areas a low level. The level of higher frequency components increases with operation time. These results are supported by the fact that, as damage to the cam follower (i.e., flaking) increases, frequency spectra decrease from ultra sonic frequency (acoustic emission) to high frequency in the audible frequency range[6]. The occurrence of high frequency components in axial vibrations after 500 hours is thus evidence of the failure of the bearing due to flaking. In particular, high frequency components increase remarkably in the peak Ⓒ. Therefore, Wigner distribution can be used as a simple diagnostic tool for the detection of high frequency components.

5. Numerical simulation

To investigate the influence of preloading or play between the cam and the cam follower in acceleration time history, the circumferential vibration of the turret was calculated using the model shown in Fig. 12. The cam follower usually contacts both side walls of the roller gear cam's taper rib. However, due to the preloading and play between the cam and the cam follower, the initial angular displacements of side walls A and B for taper rib, θ_a and θ_b, are different. The equations of motion for the circumferential vibration are as follows:

$$I_1\ddot{\theta}_1+k_3(\theta_1-\theta_3)+k_3(\theta_1-\theta_4)+k_2(\theta_1-\theta_2)+c_3(\dot{\theta}_1-\dot{\theta}_3)+c_3(\dot{\theta}_1-\dot{\theta}_4)+c_2(\dot{\theta}_1-\dot{\theta}_2)=0 \quad (1)$$

$$I_2\ddot{\theta}_2+k_2(\theta_2-\theta_1)+c_2(\dot{\theta}_2-\dot{\theta}_1)=0 \quad (2)$$

$$I_3\ddot{\theta}_3+k_3(\theta_3-\theta_1)+k_1(\theta_3-\theta_a)+c_3(\dot{\theta}_3-\dot{\theta}_1)+c_1(\dot{\theta}_3-\dot{\theta}_a)=0 \quad (3)$$

$$I_4\ddot{\theta}_4+k_3(\theta_4-\theta_1)+k_1(\theta_4-\theta_b)+c_3(\dot{\theta}_4-\dot{\theta}_1)+c_1(\dot{\theta}_4-\dot{\theta}_b)=0 \quad (4)$$

where, I_1, I_2, I_3 and I_4 are mass moments of inertia for the cam follower turret, the flywheel (load), and cam followers ① and ② respectively; k_1 and c_1 are contact stiffness and the damping coefficient between the cam and the cam follower; k_2 and c_2 are torsional stiffness and the damping coefficient of the output shaft; k_3 and c_3 are torsional stiffness and the damping coefficient between the cam follower and the cam follower turret; θ_1, θ_2, θ_3 and θ_4 are angular displacements of the cam follower turret, the output shaft, and cam followers ① and ② respectively.

In case (i), when the cam follower makes contact with both side walls of the taper rib, equations (1)-(4) are applicable to the regions $\theta_3<\theta_a$ and $\theta_4>\theta_b$.

In case (ii), when the cam follower makes contact with the side wall A of the taper rib, the following equation (5) holds instead of Eq.(4).

$$I_4\ddot{\theta}_4+k_3(\theta_4-\theta_1)+c_3(\dot{\theta}_4-\dot{\theta}_1)=0 \qquad (5)$$

Equations (1), (2), (3) and (5) are applicable to the regions $\theta_3<\theta_a$ and $\theta_4<\theta_b$.

In case (iii), when the cam follower makes contact with the side wall B of the taper rib, the following equation (6) holds instead of Eq.(3).

$$I_3\ddot{\theta}_3+k_3(\theta_3-\theta_1)+c_3(\dot{\theta}_3-\dot{\theta}_1)=0 \qquad (6)$$

Equations (1), (2), (6) and (4) are applicable to the regions $\theta_3>\theta_a$ and $\theta_4>\theta_b$.

In case (iv), the cam follower and the taper rib do not makes contact with each other. Equations (1), (2), (5) and (6) are applicable in this case.

First of all, initial angular displacements θ_a and θ_b, which are related to the magnitudes in the preload and the play, must be determined. As mentioned above, when the output shaft is in index, play always exists between the cam and the cam follower. However, since the magnitudes in preload and play can not be directly determined, θ_a and θ_b were estimated as follows. The relation of driving torque to the driving angle in the experimental indexing drive unit was measured. The driving angle was estimated in nondimentional time T (T=1.0 at a driving angle of 360°). Equations for θ_a and θ_b were established by assuming firstly that θ_a and θ_b are proportional to the driving torque, and secondly by considering four very small parameters ($\eta_1, \eta_2, \eta_3, \eta_4$) associated with the play and the preload for the theoretical angular displacement π S(T)/3 for the cam curve without play. In actuality,

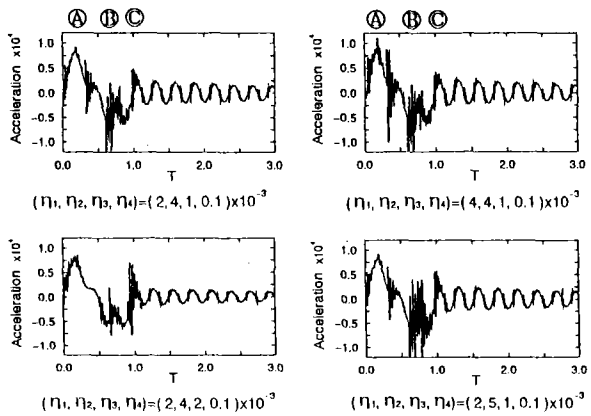

Fig.13 Calculated acceleration time histories at 600 rpm

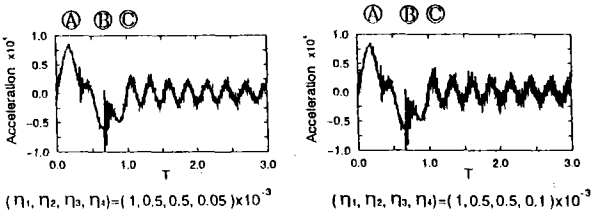

Fig.14 Calculated time histories in order to examine the influence of the failure of the cam follower on the acceleration, when the value of η_4 was taken as a random value

θ_a and θ_b were determined by dividing T into seven regions in order to approximate the measured driving torque curve. For example, θ_a and θ_b at $0\leqq T\leqq 0.18$ are represented by the following equations:

$$\theta_a=\frac{\pi}{3}S(T)-(\eta_1+\eta_4)\sin\frac{\pi}{2\times 0.19}T+\eta_4 \qquad (7)$$

$$\theta_b=\frac{\pi}{3}S(T)-(\eta_1-\eta_4)\sin\frac{\pi}{2\times 0.19}T+\eta_4 \qquad (8)$$

where S(T) is function of T.

Figure 13 shows calculated acceleration time histories at 600 rpm. The large magnitudes of η_1, η_2, η_3 and η_4 produce high frequency components in time histories. The impulsive peaks at T=0.2 , 0.65 and 1.0 correspond to the measured impulsive peaks Ⓐ, Ⓑ and Ⓒ in Fig.5 respectively. Figure 14 depicts calculated time histories, which show the influence of the failure of the cam follower on acceleration when the value of η_4 was taken as a random value. The parameter η_4 is strongly influenced by the constant terms in equations for θ_a and θ_b associated with the play, as shown in Eq.(7) and (8). The effect of η_4 can be clearly observed in time history with impulsive peaks, when the output shaft is in dwell, $T\geqq 1.0$. As a result, the increasing magnitude in the play due to wear and failure of the cam follower can be diagnosed by detecting high frequency components in the acceleration time history in dwell.

6. Conclusions

The following results were obtained from the experiment and theoretical analysis:

(1) The acceleration time histories produced by contact between a cam and a cam follower can be used to estimate the magnitude of the play in the indexing drive unit as well as the damage to the cam follower. In particular, the damage to a specific cam follower can be determined by detecting the first impulsive peaks in the time history of the acceleration in the axial direction of the output shaft.

(2) The acceleration time histories in the axial direction of the output shaft resembled those at the housing. Hence, the axial acceleration at the housing, which is easily measured, can be utilized to diagnose failure.

(3) Failure of the indexing drive could be detected and predicted through (1) the kurtosis for acceleration time histories (excluding the first and second impulsive peaks) in the axial direction of the output shaft or (2) the Wigner distribution method.

(4) The proposed nonlinear vibration model takes into consideration the play between the cam and the cam follower, and precisely simulates the actual vibration for the indexing drive. Effects of the damage to the cam and the cam follower on the acceleration time history at the housing can be estimated by the variance in the play.

References

(1) Edited by Japan steel association, Handbook of diagnostic technique for equipment, (1986), Maruzen, (in Japanese).

(2) S. Maki, Practice of machine diagnosis by vibration method, new edition, (1993), Japan plant maintenance association, (in Japanese).

(3) T. Toyoda, How to proceed the machine diagnosis, (1989), Japan plant maintenance association, (in Japanese)

(4)S. Ono, Applied design of rolling bearing, (1979), Taiga syupan, (in Japanese).